CHAPTER V. FULLERENES ANALYSIS

V.1-- BACKGROUND OF THE ALL-CARBON FULLERENE MOLECULES

V.1.1-- History

Since the development of laser-vaporization methods to produce all-carbon clusters in 1981[61], these large molecules have generated extensive interest for their unique structure. From the first observance of the remarkable resilience of C_{60} by Smalley and co-workers, the properties and stabilities of certain carbon clusters have been earnestly investigated. Largely due to mass spectrometry, a unique, icosahedral "soccerball" configuration was postulated, and in 1984 a group at Exxon[62] first observed the exclusivity of even-numbered clusters for C_n species with $n > 40$. The following year Kroto and Smalley[63] coined the term "Buckminsterfullerenes" (now simply fullerenes) for these large carbon clusters, but only microscale quantities could still be produced. Kratschmer's discovery of a macroscopic method of production by heating graphite under helium to produce a fullerene-containing soot provided a major breakthrough in fullerene synthesis[64]. Subsequent syntheses have attached metal atoms to the exterior or interior (endohedral fullerenes) of the cage, and experimentation with fullerenes is still of interest. Overall, mass spectrometry has proven vital in revealing the "unexpected and unprecedented properties"[65] of these high-mass carbon clusters.

V.1.2-- Methods of fullerene production

Several methods for fullerene production have been successful. Many laser-based techniques ablate a rotating Carbon disk with an intense, pulsed UV or visible laser. Under a high-pressure inert gas (argon, helium), the laser-induced plasma produces reactions that lead to all-carbon clustering upon supersonic cooling. Another method involves the resistive heating of graphite electrodes under an inert gas to form a "soot" of evaporated carbon clusters. A similar procedure generates a plasma through an AC or DC arc discharge using graphite rods to form the carbon soot. The pressure of the

[61] T.G. Dietz, M.A. Duncan, D.E. Powers, R.E. Smalley. *J. Chem. Phys.* **74** (1981) 6511.

[62] E. Rohlfing, D. Cox, A. Kaldvar. *J. Chem. Phys.* **81** (1984) 3322.

[63] H. Kroto, J. Heath, S. O'Brien, R. Curl, R.E. Smalley. *Nature.* **318** (1985) 162.

[64] W. Kratschmer, L. Lamb, K. Fostiropoulos, D. Huffman. *Nature.* **347** (1990) 352.

quenching gas generally controls growth size (number of carbon atoms)[66]. Fullerenes are then extracted from the soot and purified by chromatography. The fullerene products and yield are highly dependent on these extraction and purification procedures[67].

V.1.3-- Mass spectrometry and the remarkable stability of fullerenes

Mass spectrometric characterization of fullerenes has been vital since the first carbon clusters were produced. Mass spectrometry has played a key role in the discovery of fullerenes, and continues to reveal the structures and properties of these unique molecules. Although laser-ionization mass spectrometry is limited by fragmentation and cluster growth, it is said to be the best technique for reliable molecular weight distribution analysis. TOF-MS following laser desorption/ionization matches especially well for the high-mass carbon clusters, and analyses of both positive and negative ions have been performed[67,68,69]. Structural information has been obtained for ions directly emitted from the sample or by post-ionization methods[69]. Most importantly, the unlimited mass range of TOF-MS has enabled detection of photopolymerized fullerenes up to $(C_{60})_{20}$[70].

In addition, mass spectrometric investigations have revealed the remarkable stability of certain carbon clusters. Most notable, of course, is the unusual stability of C_{60}^{+} as reported by Smalley[61] and co-workers due to its unique, icosahedral, closed-shell structure. C_{70}^{+} similarly accounts for a large portion of the fullerene soot (and thus the mass spectrum) due to this ability to form a cage-like sphere. Numerous reports based on mass spectrometric observations conclude that large clusters [(C_n) with $n > 30$] only form in even-numbered units (n is even)[71,72]. Furthermore, fragmentation and growth of fullerenes for $n > 30$ occurs in C_2 units nearly exclusively, and characteristic fullerene

---

[65] S. McElvany, M. Ross. *J. Am. Soc. Mass Spectrom.* **3** (1992) 268.

[66] E. Rohlfing. *J. Chem. Phys.* **93** (1990) 7851.

[67] W. Creasy, J. Zimmerman, R. Ruoff. *J. Phys. Chem.* **97** (1993) 973.

[68] S.Y. Wang, L. Zhu, Jian-Zhong Lu, Pei-Nan Wang, Yu-Fen Li. *Chinese Science Bulletin.* **39** (1994) 469.

[69] P. Wurz, K. Lykke, M. Pellin, D. Gruen, D. Parker. *Vacuum.* **43** (1992) 381.

[70] D. Cornett, I. Amster, M. Duncan, A. Rao, P. Eklund. *J. Phys. Chem.* **97** (1993) 5036.

[71] J. Zimmerman, J. Eyler, S. Bach, S. McElvany. *J. Chem. Phys.* **94** (1991) 3556.

[72] D. Lineman, K. Somayajula, A. Sharkey, D. Hercules. *J. Phys. Chem.* **93** (1989) 5025.

mass spectra portray peak differences of 24 amu. In addition to C_{60} and C_{70}, other "magic number" fullerenes exhibit special stability. The stable structures of C_{74}, C_{76}, C_{78}, C_{82}, and C_{84} seem to account for their enhanced presence in the soot over other even-numbered clusters.

V.1.4-- Controversy of gas-phase formation versus true sample constitution

The crucial question of maintaining sample integrity during fullerene analysis is especially problematic with laser-ionization mass spectrometry, and this "true sample constituents versus gas-phase products" controversy has been widely noted[67,70,73,74,75,76]. Primarily, it has been "well known"[67] that laser ablation of non-fullerene containing materials can produce fullerenes under mass spectrometric conditions through gas-phase growth in the laser-induced microplasma at the sample surface[66,76]. Pure C_{60} samples likewise suffer from these gas-phase aggregations to generate larger fullerenes, and there is thus the question of whether the mass spectrum of a particular pure or soot sample represents the actual components of the specimen. In addition to these growth processes, laser-induced photofragmentation is common especially for ultraviolet lasers, as fullerenes absorb strongly at these wavelengths. The mass spectrometer therefore detects any true-sample ions, fragment ions, and aggregate ions that are present in the microplasma.

Several laser-ionization mass spectrometric methods commonly address the problem of representative sampling. Because fullerene production is largely dependent on the ablation conditions, the mass spectral dependence on laser fluence can be probed. "Soft" laser desorption/ionization, using the minimum laser power for ion production, reduces laser-generated fragmentation and aggregation products to provide more representative sampling. Slight increases in laser energies above the threshold for ion production, however, often fragment the fullerene ions[74]. Higher fluences promote gas-phase ion-molecule reactions leading to cross-linking[70], aggregation, and $(C_{60})_n$

[73] D. Parker, K. Chatterje, P. Wurz, K. Lykke, M. Pellin, L. Stock, J. Hemminger. *Carbon.* **30** (1992) 1167.

[74] A. Herod, B. Stokes. *J. Chem. Soc. Perkin Trans. 2.* **3** (1994) 499.

[75] G. Ulmer, E. Campbell, R. Kuhnle, H. Busman, I. Hertel. *Chem. Phys. Lett.* **182** (1991) 114.

[76] R. Beck, P. St. John, M. Alvarez, F. Diedrich, R. Whetten. *J. Phys. Chem.* **95** (1991) 8402.

dimerization/trimerization. Therefore, carefully maintaining threshold laser intensities on the sample maximizes reliable compositional analysis.

Instrumental configurations also address the controversy of representative sample species versus laser-generated products. Mass spectrometric comparison of both the positive- and negative-ion spectra isolate actual sample components. Growth and fragmentation distributions in positive-ion spectra are observed more readily than in analogous negative-ion spectra following laser-ablation[67,68,77]. Mechanistically, justification of this observation confirms that negative-ion mass spectra should be more characteristic of the actual sample. Because the electron affinity of the fullerenes is less than the energy needed to fragment the molecule, a cluster with sufficient energy to fragment likewise has sufficient energy to lose the extra electron and neutralize to an undetectable species. Furthermore, the added energy (decreased stability compared to C_{60}^{+}) of aggregate ions tends to detach the extra electron leading again to neutralization[67]. Therefore, both negative ion fragments and aggregates are less likely to be detected by mass spectrometry than their positive ion counterparts. Furthermore, a higher laser intensity threshold for positive ion production (10.9 $\mu J/mm^2$) in comparison to negative ions (5.7 $\mu J/mm^2$) increases the likelihood of gas-phase reactions accompanying positive ion generation. For these considerations, the negative-ion spectrum should better represent the true species in the sample, and comparisons of both the positive-ion and negative-ion spectra may elucidate ionization mechanisms.

V.2-- GOALS OF OUR FULLERENES ANALYSIS

Fullerene samples exploit the high-mass range of the LI-TOF-MS technique. These investigations will challenge the ability of our new instrument to generate mass spectra and calibrate spectral peaks through 2500 amu. Sample preparation methods will be studied for these solution-samples as well. Furthermore, the pure C_{60} and impure C_{70} "soot" samples can be compared to gain insight into the controversial issue of gas-phase aggregation versus true sample composition.

[77] E. Millon, J. Weber, B. Kubler, J. Theobald, F. Muller. *Analusis.* **21** (1993) 319.

V.3-- SAMPLES ANALYZED AND SAMPLE PREPARATION

Two different fullerene samples were obtained as solids from Dr. Harry Dorn and his research group at Virginia Polytechnic Institute and State University (VPI&SU). The first, a C_{60} sample, was purified by chromatography prior to analysis and believed to contain only C_{60}. The second, referred to as a "C_{70} soot", is a sample of arc-produced soot without extensive purification. Believed to contain higher quantities of non-C_{60} species, it allows a comparison of a "pure" sample and an "impure" extract.

Samples were deposited as a "slurry" onto a 1/32-inch thick aluminum disk that was attached to the sample probe. Several volatile solvents (acetone, ethanol, and toluene) were investigated for their ability to solubilize the fullerenes, and toluene was chosen for sample preparation. Several micrograms of the fullerene sample were dissolved in a minimal amount of toluene and placed via micropipette onto the aluminum disk in an area of approximately 0.25 cm^2. The solvent was allowed to evaporate to provide the solid slurry sample, and the probe was inserted into the mass spectrometer. Laser ablation was performed as with previous samples by focusing the laser beam through a 25-cm focal length lens to create a spot radius on the sample slurry of ~11 μm.

V.4-- C_{60} RESULTS

The initial goal of verifying instrument reliability in higher-mass regions was clearly achieved. Optimization of the TOF-MS, especially increasing the repeller pulse delay to ~40 μs, allowed sharp signal improvements for the C_{60}^+ ion (720 amu). Resolution of most spectra ($t/2\Delta t_{FWHM}$) was at least several hundred; however, resolution limitations precluded isotope separation (i.e. $^{12}C_{59}{}^{13}C_1^+$, $^{12}C_{58}{}^{13}C_2^+$, etc.) and resulted in a tailing of the C_{60}^+ peak toward longer times-of-flight following the centroid. Mass calibration accuracies from C_1 (12 amu) through the largest fullerene observed, ~C_{270} (~3243 amu), were approximately 0.1%. As also observed by others[75], the best signal was obtained by ablating a fresh sample surface, and the ion intensity decreased rapidly upon prolonged ablation of the same location. Up to fifty laser shots could be averaged

per spectrum to improve the S/N ratio without a significant loss of signal intensity. In most cases, the average of 50 shots was used to acquire a mass spectrum, and the sample probe was rotated slightly to expose a new sample surface for each spectrum.

Regardless of the laser energy, C_{60}^+ was the most prominent species observed. Although some difficulties such as the "fresh spot" phenomenon arose when trying to gather reproducible data on the relation between ion yield and laser energy, distinct trends were observed. The threshold for fullerene ion production (ion signal at least 1 mV when the detector gain ~10^5) was ~1-2 μJ, and at this intensity C_{60}^+ was the only observed ion. Slightly more intense beams above the threshold (~4 μJ) fragmented C_2 units from the C_{60}^+ to generate C_{58}^+ and C_{56}^+ peaks, as Figure V.1 portrays, and such ease of dissociation upon laser beam impact is common[68,75]. A further energy increase to ~7 μJ yielded aggregate peaks centered around C_{120}^+ (See Figure V.2) and some C_{70}^+ in other spectra. As shown in Figure V.3, laser fluences from ~10-15 μJ significantly increased the ion yield for peaks from C_{56}^+ to C_{70}^+ as well as the dimers (~C_{120}^+). Noteworthy is the sharp decrease in ion production for species following C_{70}^+ until the next modal increase beginning ~C_{100}^+. Very high energy densities (over ~15 μJ) produced nearly continual distributions in C_2 units of fullerene clusters from C_{50}^+ to C_{240}^+ and higher, with a trimodal distribution of the aggregates, peaking at ~C_{60}^+, ~C_{120}^+, and ~C_{180}^+. At these higher laser energies, prolonged ablation of the same sample spot (over ~300 laser shots) decreased the intensities of the aggregate peaks and yielded significant signals only from the C_{60}^+ and C_{70}^+ ions.

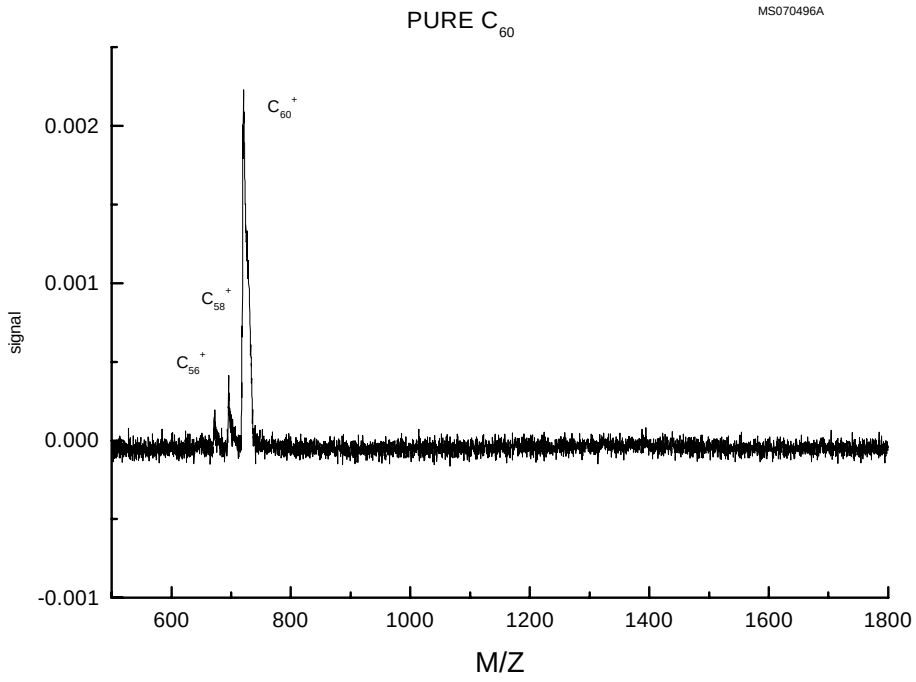

Figure V. 1: Low laser energy ablation of the pure C_{60} sample.

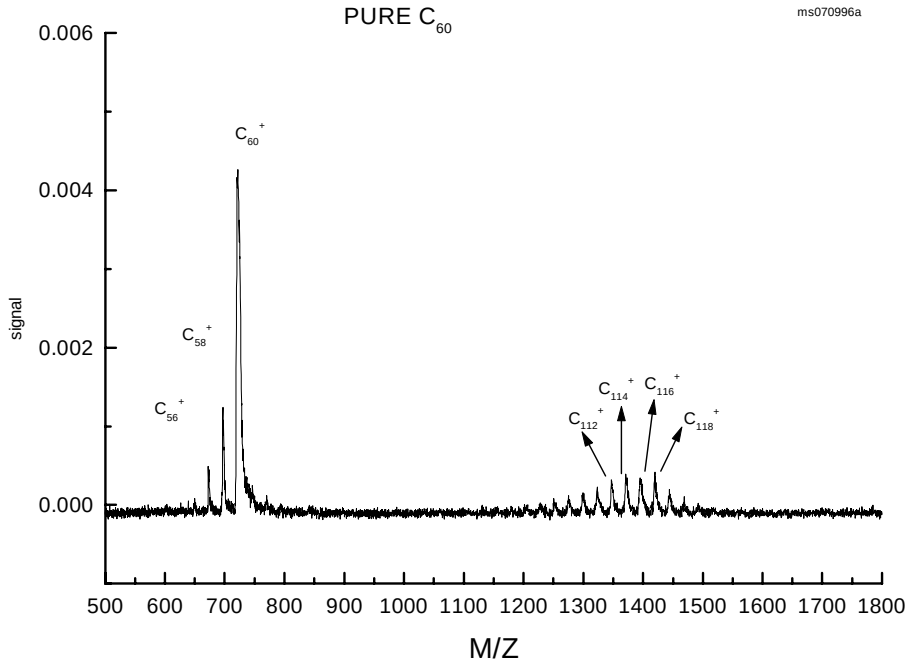

Figure V. 2: Moderate laser energy ablation of the pure C_{60} sample.

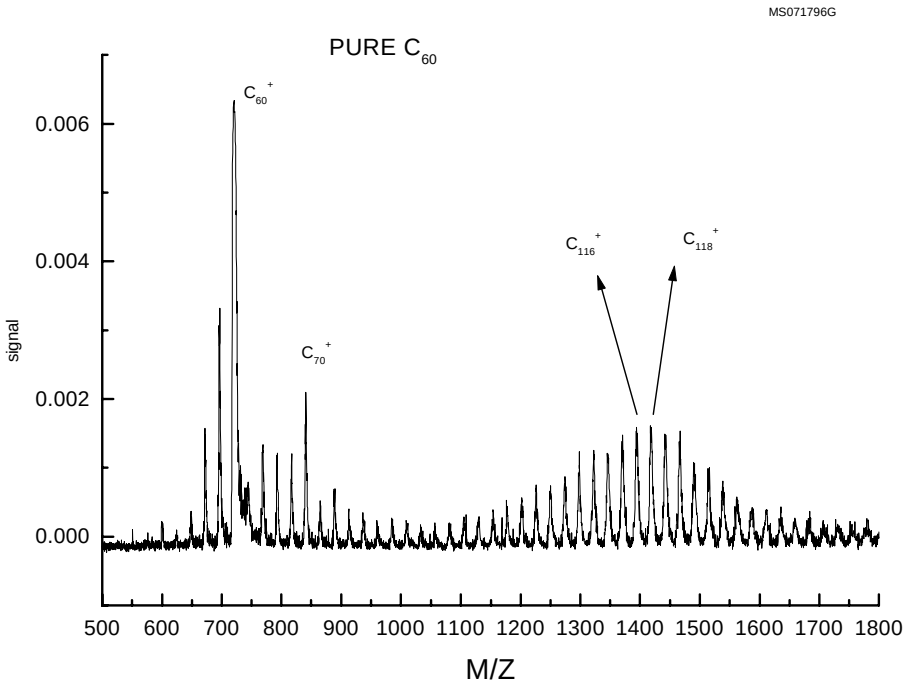

Figure V. 3: High laser energy ablation of the pure C_{60} sample.

V.5-- C_{70} RESULTS

For the impure soot ("C_{70}") sample, the LI-TOF-MS again reliably ionized and detected the high-mass species. The ablation of a fresh surface greatly increased the intensities of all species observed, and repeated ablation at the same location decreased the ion signal. Spectra were acquired as the average of 50 laser shots for improved S/N ratios. In most cases, repeller delay times and TOF-MS conditions were similar to the C_{60} sample.

This soot sample provided quite a rich spectrum of fullerene peaks. The most prominent signals arose from the C_{60}^+ species for all laser energies. The threshold laser energies for observation of any species was 1-2 μJ, and at this energy only low-intensity $C_{60}^+$and C_{70}^+ peaks could be observed (S/N of only ~2). A slight increase in laser energy to 4-5 μJ, however, revealed a variety of fullerene peaks, as is shown in Figure V.4. In contrast to the C_{60} sample, noteworthy signals from C_{56}^+, C_{58}^+, C_{68}^+, C_{74}^+, C_{76}^+, C_{78}^+, C_{82}^+, and C_{84}^+ in addition to the most intense C_{60}^+ and C_{70}^+ are clearly visible at S/N ratios of over 10. Like the C_{60} sample, aggregate formation in units of C_2 accompanied increased laser energies (~7 μJ), with the progression from ~C_{110}^+ to C_{130}^+ exhibiting enhanced intensities over nearby ions (See Figure V.5). The "falloff" after C_{84}^+ before the polymerized species (~C_{110}^+) is noteworthy, and has been observed by others[75]. This observation contrasts the sharp falloff after C_{70}^+ and lack of C_{74}^+ to C_{84}^+ peaks that were observed under similar laser ablation conditions of the pure C_{60} sample. Higher laser energies (>15 μJ) increased the signal intensities of all species produced from the C_{70} soot sample and often saturated the C_{60}^+ and C_{70}^+ peaks. The trimodal distribution (~C_{60}^+, ~C_{120}^+, and ~C_{180}^+) as seen with the pure C_{60} sample was again observed (See Figure V.6). Aggregate clusters up to ~C_{270}^+ were occasionally produced at these intense laser fluences.

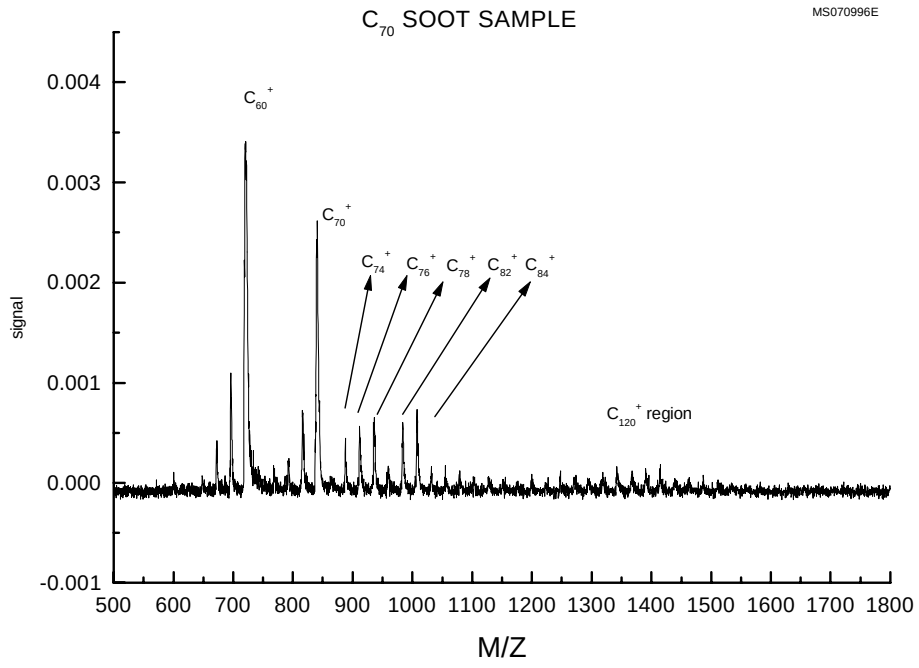

Figure V. 4: "Magic number" ion peaks for low laser energy ablation of the C_{70} soot.

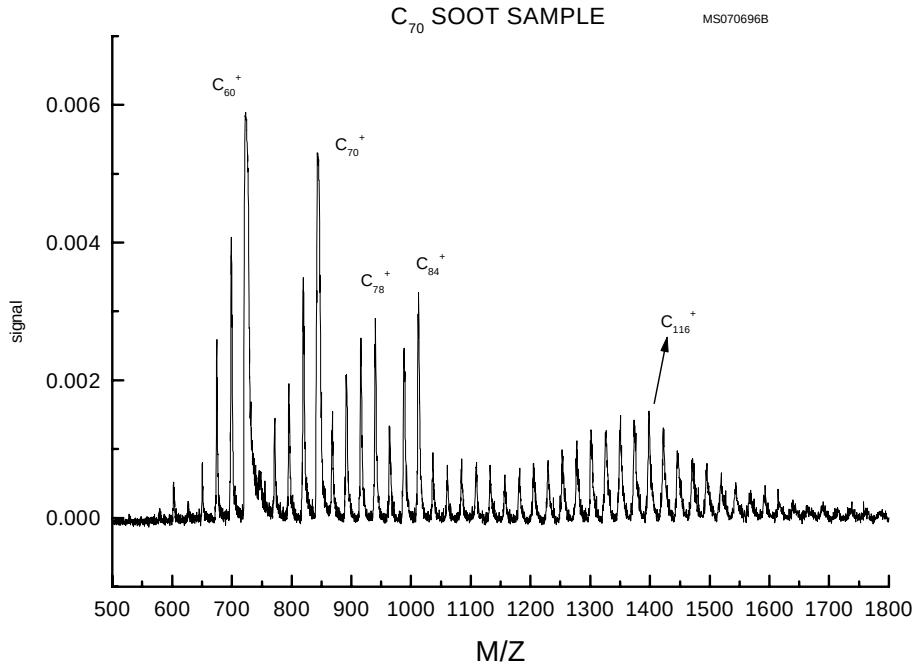

Figure V. 5: Moderate laser energy ablation of the C_{70} soot.

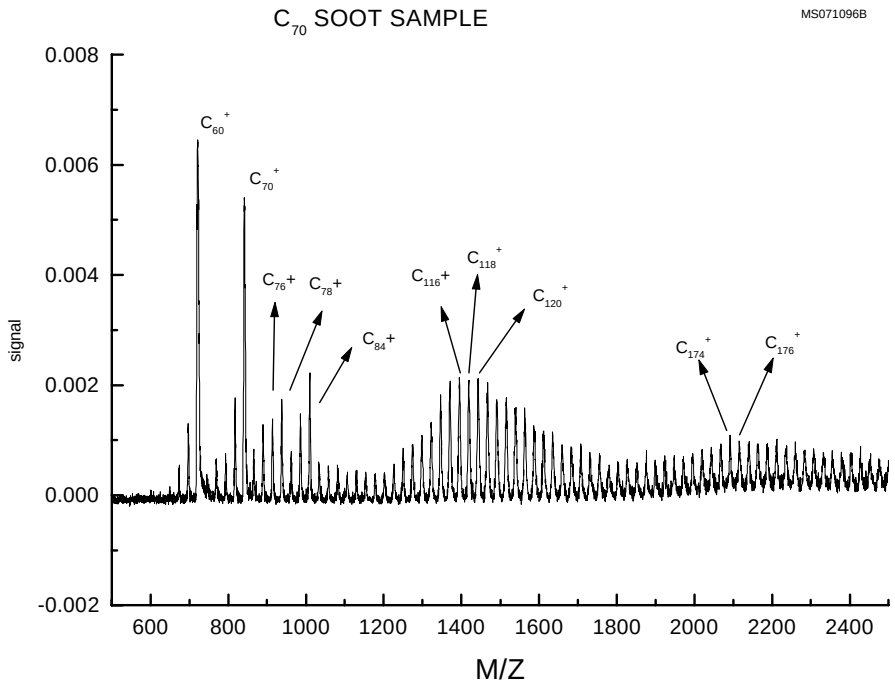

Figure V. 6: High laser energy ablation of the C_{70} soot.

V.6-- DISCUSSION

At sufficiently high energies, it is clear that the laser ablation process generates a variety of species in the gas phase from even the pure C_{60}. With the extraction pulse delay required (>30 μs) for the ions to rise from the sample surface to the flight tube axis, there appears ample time for fragmentation and gas-phase reactions such as the clustering which was observed at the higher laser energies. Since the ionization potentials of the fullerenes are quite similar, the conformational stability governs the ion yield of these gas-phase products.

The strict adherence to the "even number" rule as observed in the experimental data has been attributed to this enhanced stability issue. In fact, Hercules[72] notes that C_n (n even) products are nearly exclusive for n greater than 30 as large, odd-numbered fullerenes suffer from increased spherical strain. However, for n < 30, the decreased size of the fullerene species allows for stable formations of odd-numbered species. To test this issue, the TOF-MS was optimized for detection of lower masses (under ~300 amu) by decreasing the repeller delay. Although an increased laser energy (over ~15 μJ) was necessary for their production, odd-numbered species were observed (See Figure V.7). In addition, isotope resolution was achieved, as Figure V.8 shows the separation of $^{12}C_9{}^{13}C_1{}^+$ and $^{12}C_8{}^{13}C_2{}^+$ with S/N ratios of approximately 4 and 2, respectively.

The experimental observation of the larger ~C_{120} dimer/cluster ions, most likely produced by the high-energy fragmentation of C_{60} followed by re-aggregation, is quite common in laser ablation studies of fullerenes[67, 70, 73,76]. Although confirmation of the exact structure is difficult, two possibilities have been postulated, an "expanded cage" configuration or an external linking of two C_{60} cages together[70]. The $C_{120}{}^+$ peak, however, was not the most intense of this distribution (from ~$C_{110}{}^+$ to $C_{126}{}^+$). In most cases, the distribution maximized at slightly lower-mass cages, $C_{116}{}^+$ or $C_{118}{}^+$, although similar ion intensities for $C_{116}{}^+$ to $C_{120}{}^+$ were common. By analogy to the $C_{60}{}^+$ peak dominating the spectra, it would seem that the $C_{120}{}^+$ peak should provide the maximum signal for the aggregate progression ~$C_{110}{}^+$ to $C_{126}{}^+$. However, the production of a $C_{120}{}^+$ species by linking two C_{60} units may be less likely than expected due to the enhanced stability of $C_{60}{}^+$ by itself. With our results, therefore, the double-cage structure

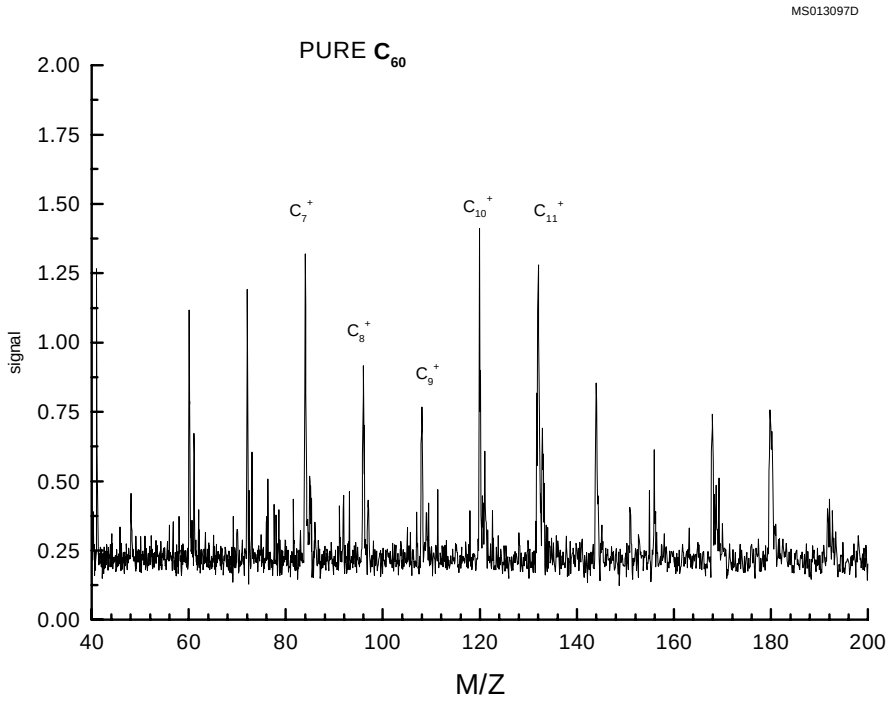

Figure V. 7: Odd-numbered low-mass fullerenes.

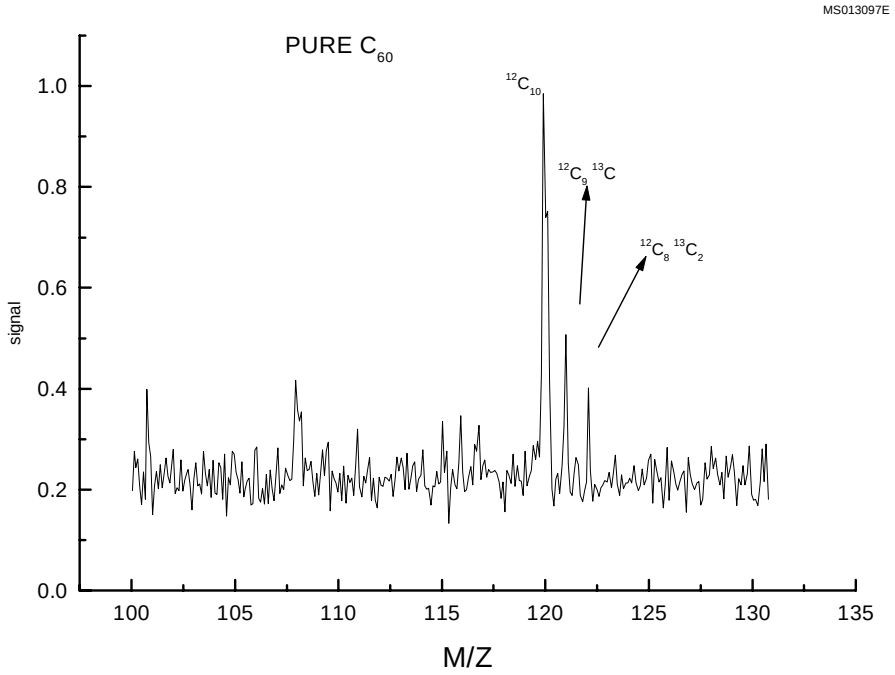

Figure V. 8: Isotope resolution for low-mass fullerenes.

(two C_{60} units) seems less likely than a polymerization to an expanded cage. A more common ion-molecule reaction could be a fragment such as C_{58}^+ joining with the stable C_{60}[71]. Such ion-molecule reactions of one C_{60} and a fragment ion would indeed account for the abundant C_{118}^+ and C_{116}^+ contributions to the spectra. An analogous argument could be made for the trimer (C_{180}) region of the mass spectrum. Again, ion yields for the peaks slightly smaller than C_{180}^+ were more abundant than the $(C_{60})_3^+$. Three separate C_{60} units linked externally thus seems less likely than a re-aggregation of C_{60} and fragments to account for the increased intensities of the C_{174}^+ to C_{178}^+ that were observed.

V.7-- ACTUAL SAMPLE CONSTITUENT VERSUS GAS-PHASE FORMATION ISSUE

Because both "pure" C_{60} and "impure" C_{70} soot samples were analyzed under similar conditions, insight into the sample integrity controversy can be obtained. As noted previously, the laser energy required for C_{60}^+ production from the pure C_{60} sample could be reduced so that it was the only peak in the spectrum. With the ionization potentials of the other possible fullerene components quite similar, one would expect the nearly simultaneous ionization of other sample components as well. For the pure C_{60}, however, other fullerenes were not observed until the laser energy was increased. Furthermore, fragmentation to C_{58}^+ and C_{56}^+ preceded the production of masses over C_{60}. The possibility does exist that C_{58} and C_{56} are actual sample constituents, but it is unlikely that they would account for as large a proportion of a fullerene extract as the more stable C_{70}[73,75]. For higher laser fluences, there is the observance of C_{70}^+, but accompanying this peak is a significant higher-mass distribution centered around C_{120}^+. The C_{120}^+ ions, produced only in gas-phase aggregation and not by the ionization of true sample components, confirm that gas-phase formation is occurring. The most likely conclusion, therefore, is that these high-energy spectra are not representative of the actual sample. The C_{70}^+ and other ions that were not observed at threshold-level laser energies are probably gas-phase products from a relatively pure C_{60} sample.

In the C_{70} soot sample, analysis of the ion yield dependence on laser energy and a comparison with the C_{60} data reveal a high likelihood of other fullerenes in the sample itself. Most importantly, identification of the magic number species (C_{74}, C_{76}, C_{78}, C_{82},

C_{84}) precedes the appearance of the dimerized aggregates (~C_{120}^{+}), as shown in Figure V.4). Comparing this spectrum with the simpler spectra of C_{60} under similar conditions (Figure V.1), the predominance of magic number species in the soot spectra shows they are true sample components. If they were gas-phase products, we would have expected their formation from the pure C_{60} sample as well under the same low-energy conditions. One possibility is that gas-phase aggregation is somehow deterred or undetectable in the C_{70} analysis, but this is clearly not the case. Figures V.5 and V.6 reveal that dimers and trimers could be produced and detected in gas-phase aggregation of the C_{70} soot. As a final confirmation, two high-energy ablation spectra (See Figures V.3 and V.6), which both portray polymerized aggregates, should be compared. The relative abundance of the C_{74} – C_{84} "magic number" ions to the ~C_{120}^{+} peaks in the C_{70} sample (Figure V.6) is visibly much greater than in the pure C_{60} sample (Figure V.3). Thus, it is most likely that large proportions of C_{70}, C_{74}, C_{76}, C_{78}, C_{82}, C_{84}, in addition to C_{60}, truly comprise the soot sample.

V.8-- QUANTITATION OF SPECIES IN THE C_{70} SOOT

Assuming the "magic number" species C_{74}, C_{76}, C_{78}, C_{82}, and C_{84} are indeed actual constituents of the soot sample, quantitation of the relative amounts of each are important for compositional analysis. To ensure the integrity of the actual sample and minimize gas-phase species formation, the laser energies were maintained at the threshold for the "magic number" production. Fifteen spectra, each compiled from the average of 50 laser pulses, were obtained, and a fresh sample location ablated for each spectrum. Relative amounts of each of these as well as C_{60}^{+} and C_{70}^{+} were determined based on peak height data. The results are highlighted in Table V.1, which depicts the ratio of the given ion to the C_{70}^{+} peak.

The most stable fullerene, C_{60}, comprises the majority of the sample, with abundance greater than 125% of the C_{70} product. The other constituents are present in quantities ranging from ~25% to 44% of the C_{70} fullerene. It is apparent that the precision of the measurements is low (%RSD values range from 13% to 77%), as was observed also in the quantitation of the ion yields discussed in Chapter III. Perhaps it is more informative to omit the much more abundant C_{60}^{+} and C_{70}^{+} yields, and concentrate

on just the other “magic numbers”. Table V.2 shows the same data, but ratioed to C_{78}^+ to give the relative amounts of just these prominent fullerenes.

The %RSD in these ratios is lower due to the proximity of the ratios to each other, as opposed to the low ratios when comparing the yield to C_{70}^+. The deviations are still up to 48%, but this data reveals more clearly that the most abundant of the non-C_{60} and non-C_{70} fullerenes are C_{78} and C_{84}. All of the main constituents of the soot listed in Table V.2 are at least 75% of the C_{78} product.

Table V. 1: "Magic number" fullerenes in the C_{70} soot sample (ratioed to C_{70}^+).

SPECIES	C_{60}^+	C_{70}^+	C_{74}^+	C_{76}^+	C_{78}^+	C_{82}^+	C_{84}^+
MEAN RATIO	1.27	1.00	0.34	0.26	0.41	0.30	0.44
%RSD	13.24	0	77.29	78.68	44.51	65.18	39.64

Table V. 2: "Magic number" fullerenes in the C_{70} soot sample (ratioed to C_{78}^+).

SPECIES	C_{74}^+	C_{76}^+	C_{78}^+	C_{82}^+	C_{84}^+
MEAN RATIO	0.86	0.76	1.00	0.81	1.06
%RSD	46.3	48.16	0	38.24	14.6